Direct growth of highly oriented GaN thin films on silicon by remote plasma CVD

Lisa Watrin, François Silva, Cyril Jadaud, Pavel Bulkin, Jean-Charles Vanel, Dominique Muller, Erik V. Johnson, Karim Ouaras, Pere Roca I Cabarrocas

Direct growth of highly oriented GaN thin films on silicon by remote plasma CVD

Lise Watrin [1,2], François Silva [2], Cyril Jadaud [2], Pavel Bulkin [2], Jean-Charles Vanel [2], Dominique Muller [3], Erik V. Johnson [2], Karim Ouaras[2], and Pere Roca i Cabarrocas [1,2,a)]

[1]Institut Photovoltaïque d'Ile-de-France (IPVF), 18 Boulevard Thomas Gobert, 91120 Palaiseau, France
[2]LPICM, CNRS, École Polytechnique, Institut Polytechnique de Paris, route de Saclay, 91120, Palaiseau, France
[3]Laboratoire ICube, Université de Strasbourg et CNRS, 23 rue du Loess, 67037 Strasbourg Cedex 2, France

[a)] Electronic mail: pere.roca@polytechnique.edu

Abstract. We report on low-temperature (500°C) and low-pressure (0.3 mbar) direct growth of GaN thin films on silicon (100) substrates using Remote Plasma Chemical Vapor Deposition (RP-CVD). In the custom-designed reactor, an RF Inductively Coupled Plasma (ICP) is generated remotely from the substrate's area to facilitate the decomposition of group-V precursor, N_2 with added H_2, while group-III precursor Trimethylgallium (TMGa), is directly injected into the growth chamber mixed with H_2 carrier gas. Growth parameters such as RF power, process pressure and gas flow rates have been optimized to achieve a film growth rate of about 0.6 µm/h. Several characterization techniques were used to investigate the plasma and the properties of the grown thin films in terms of their crystallinity, morphology, topography, and composition. The films are highly textured with a preferential orientation along the c-axis of the wurtzite structure. They present a small roughness in the nanometer range and a columnar microstructure with a grain size of one hundred nanometers, and a gallium polarity (+c plane oriented). RBS and NRA analysis show that the chemical composition is homogeneous through the depth of the layer, with a

III/V ratio close to 1, a very low content of oxygen (below the detection limit ~1%) and a carbon content up to 11%. It was shown that that the increase of plasma power helps to reduce this carbon contamination down to 8%. This research paves the way for a growth method compatible with cost reduction of III-V thin film production achieved through reduced gas consumption facilitated by RP-CVD operation at low pressure.

I. INTRODUCTION

Since the emergence of white LEDs was made possible by the development of blue LEDs based on gallium nitride (GaN), for which the 2014 Nobel Prize in Physics was awarded to Nakamura, Amano and Akasaki[1], this material from the III-Nitride family has completely revolutionized several sectors of semiconductor industry. Indeed, this wide band-gap semiconductor (3.4 eV at room temperature) combines many advantages such as a low dielectric constant, a high thermal conductivity, and a high electron mobility to name but a few, which makes it indispensable for power electronics and optoelectronic devices (light-emitting diodes, lasers, transistors, photodetectors, solar cells, etc...)[2]. It is notably the material of choice for emitting or detecting devices that require to operate in wavelength range spanning from ultraviolet to blue[3,4]. Moreover, thanks to both its high resistance to radiation and harsh environments owing to its good chemical stability, it is also well suited for high-power and high temperature applications[5].

The most widely used techniques for the deposition of GaN thin films are MetalOrganic Chemical Vapor Deposition (MOCVD) and Molecular Beam Epitaxy (MBE)[6], however, they suffer from the drawback of being both costly and complicated as

they involve very high pressure (~500 mbar) or ultrahigh vacuum, respectively. Plasma-assisted growth, such as in the case of plasma-enhanced chemical vapor deposition (PECVD), offers a more cost-effective method in which a plasma discharge is used to dissociate precursors at intermediate pressure (0.1-1 mbar)[7]. Since this technique allows working at reasonably low pressure, the consumption of precursors which is, along with the substrate, the main source of costs in CVD[8], can be considerably reduced.

PECVD is commonly used for the industrial production of silicon-based materials[9–11]. Some studies showing the feasibility of plasma-assisted processes for III-V semiconductors deposition were published in the 1980s[12] and the subject is again attracting interest[13–15] due to the strong growth of the III-V semiconductor market. Remote Plasma CVD (RP-CVD) is a branch of the PECVD family, with the distinctive feature of having a plasma located away from the substrate, thus preventing ion bombardment effects. It is also a process that is operated at a lower temperature than conventional CVD. This may result in higher quality films, as defects due to thermal stress can be reduced. Moreover, it also gives the opportunity to grow on temperature-sensitive substrates, for flexible applications in particular.

The key advantage of RP-CVD lies on the efficient dissociation of challenging-to-crack gas precursors such as N_2, generating highly reactive species within the plasma. Consequently, we can conduct depositions at significantly lower temperatures which is, for instance, particularly beneficial to avoid undesirable reactions occurring at high temperatures (e.g. meltback etching which occurs in the case of contact between a gallium-based material and a silicon substrate[16]). With the interest generated by research into

reducing the cost of III-V materials growth in recent years, some teams have begun to develop such processes for III-V growth[17–20].

One of the major challenges in growing GaN is to find a substrate that fits its structure. Due to the lack of bulk GaN wafers, the substrates most frequently employed for the heteroepitaxy of GaN are sapphire (Al_2O_3), aluminum nitride (AlN) and silicon carbide (SiC). Unfortunately, these materials are not economically competitive, and have the disadvantage of being insulating in nature and not available in large diameter which make them poor candidates for high-volume production of high-power devices[21]. Silicon (Si) became an interesting candidate as a substrate for GaN growth when the first GaN LED grown on Si was demonstrated via MBE[22,23], which proved that functional devices could be fabricated on it. Silicon can meet the requirements of a low-cost, large-area, and conductive substrate and would thus allow the integration of high-power GaN optoelectronic or electronic devices with Si-based electronics. However, this remains very challenging given the lattice mismatch between Si and GaN of nearly 16% (leading to a significant dislocation density in the GaN layers), and the thermal expansion coefficient mismatch, which amounts to 54% and can induce mechanical stress in the epitaxial layers, leading to cracking and delamination.

In this study, we demonstrate that highly textured GaN thin films can directly be grown on low-cost silicon substrates using a remote inductive coupled plasma operating at RF power of 250 W. The growth was performed at a pressure of 0.3 mbar and a temperature of 500°C. In section II, we present the custom-built RP-CVD reactor and the various solid-state characterizations techniques that were used. In section III, we will present the results

related to the main features of the plasma and those of the GaN films, in terms of crystalline structure, morphology and composition.

II. EXPERIMENTAL

A. RP-CVD reactor set-up

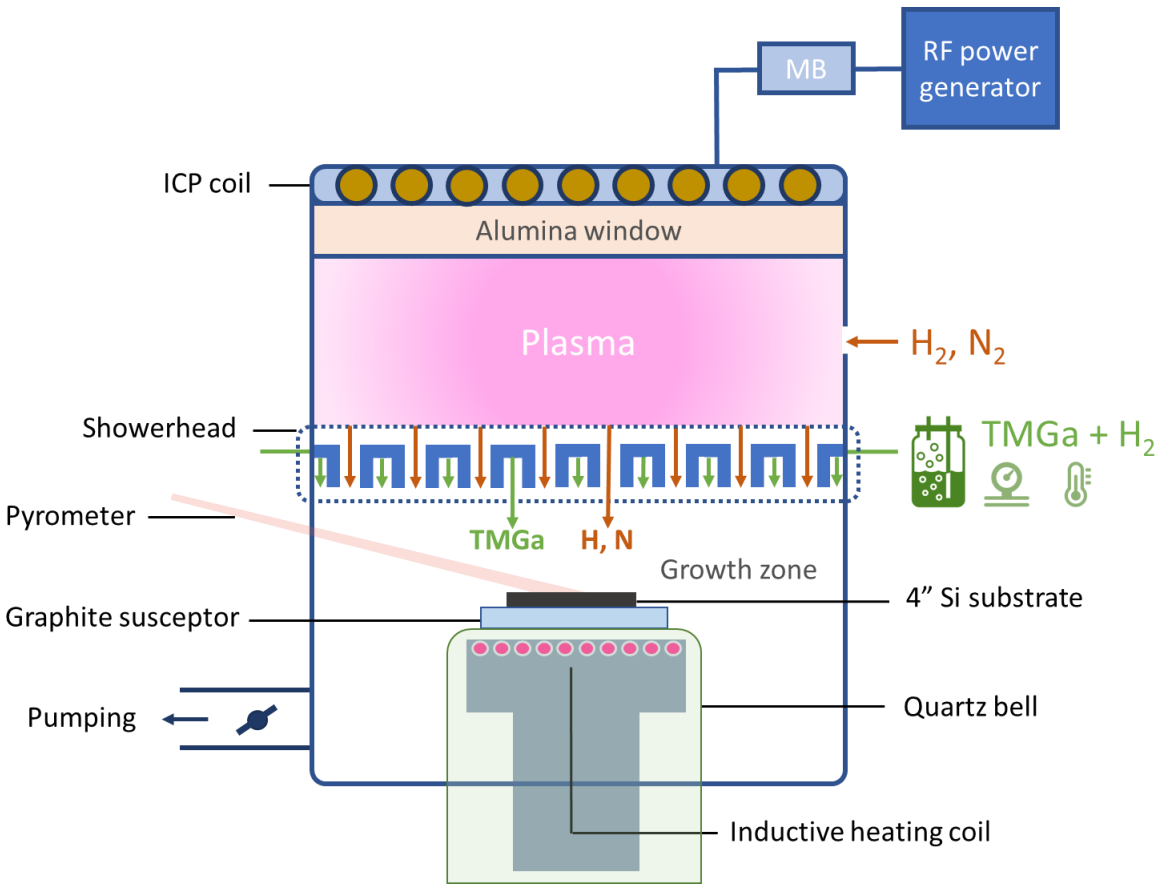

Figure 1. Schematic representation of the RP-CVD reactor.

Figure 1 is a schematic of the in house custom designed RP-CVD reactor used for the growth of GaN layers. The inductive coupled plasma (ICP) is generated by a flat coil antenna powered by a 13.56 MHz radiofrequency (RF) generator (Cito, COMET)

connected to a matching box (MB). An alumina window allows to transmit the electromagnetic RF field to the discharge zone. The group V precursor, nitrogen (N_2) diluted in hydrogen (H_2), is introduced in the plasma zone above the showerhead for dissociation into N-atom radicals that then pass through the showerhead toward the growth zone. Nitrogen was chosen over ammonia for simplicity of use as ammonia is toxic and corrosive. Nevertheless, it is well known that N_2 is very difficult to crack as the dissociation energy of this molecule stands at 946 kJ/mol[24]. Therefore, an ICP source was used, given its efficiency at dissociating N_2 when operating in the bright mode (H-mode)[25].

The group III precursor trimethylgallium (TMGa) and its carrier gas, namely hydrogen (H_2) are directly injected into the showerhead toward the growth chamber (see **Figure 1**). Injecting trimethylgallium away from the plasma prevents over-dissociation of methyl radicals that would lead to deterioration of the layer through carbon contamination. The reactions between the group III and V species then proceed in the growth zone, at the level of the heated substrate. The substrate holder is composed of a stainless-steel base surmounted by a quartz bell protecting the inductive heating system, fitted with a quartz spacer on top of which a graphite susceptor coated with a thin layer of SiC can receive substrates as large as 4 inches in diameter. Inductive coupling is employed to ensure a local heating at the substrate, which is crucial to avoid decomposition of TMGa and subsequent gallium contamination on the wall surfaces. The substrate temperature is controlled via a regulation unit (Master Controller v3+, CEIA) and monitored with a pyrometer (SH15/SLE, CEIA). After deposition, a motorized translation allows the substrate holder to be moved out to a loadlock through which the sample is picked up or loaded.

B. Deposition process of GaN on c-Si

Depositions were performed on 4-inches (100) p-type silicon substrates, doped with boron ($\rho \approx 0.001$ Ohm.cm). The native oxide layer on the bare wafers was removed by performing a 30 seconds dipping into a bath with hydrofluoric acid (HF) diluted to 5% with deionized water. The substrate was then immediately loaded into the reactor. The chamber was pumped to a base pressure of around 3.10^{-7} mbar. Under vacuum, the substrate temperature was gradually increased (~100°C/minute). Prior to deposition, a plasma treatment was applied to the silicon substrate to remove organic contaminations from its surface. It consisted of a H_2 plasma (100 sccm) at 150 W of RF power under a pressure of 0.3 mbar, lasting 10 minutes [26]. In order to determine the optimal conditions that ensure both a high growth rate and a film of high crystalline quality, we performed a parametric study by varying the growth temperature, the substrate's surface state (i.e. with or without nitridation) and the plasma power (**Table 1**). **Figure 2** shows the results of the optimization of the process parameters in terms of growth rate.

Sample name	**Substrate temperature**	**Chamber pressure**	**RF plasma power**	**Group-III precursor TMGa flow / H_2 flow**	**Group-V precursor H_2 flow/ N_2 flow**
S1	300°C	0.5 mbar	150 W	2 sccm / 60 sccm	10 sccm / 400 sccm
S2	400°C	0.5 mbar	150 W	2 sccm / 60 sccm	10 sccm / 400 sccm
S3	500°C	0.5 mbar	150 W	2 sccm / 60 sccm	10 sccm / 400 sccm
S4	500°C	0.5 mbar	150 W	2 sccm / 60 sccm	10 sccm / 400 sccm
S5	500°C	0.3 mbar	150 W	1 sccm / 30 sccm	5 sccm / 200 sccm
S6	500°C	0.3 mbar	200 W	1 sccm / 30 sccm	5 sccm / 200 sccm
S7	550°C	0.3 mbar	200 W	1 sccm / 30 sccm	5 sccm / 200 sccm
S8	600°C	0.3 mbar	200 W	1 sccm / 30 sccm	5 sccm / 200 sccm
S9	**500°C**	**0.3 mbar**	**250 W**	**1 sccm / 30 sccm**	**5 sccm / 200 sccm**
S10	550°C	0.3 mbar	250 W	1 sccm / 30 sccm	5 sccm / 200 sccm
S11	500°C	0.3 mbar	300 W	1 sccm / 30 sccm	5 sccm / 200 sccm

Table 1. Growth conditions for 11 samples of GaN thin films produced by RP-CVD. S9 conditions have been chosen for the detailed characterization of the film in section III.

Samples from S1 to S3 illustrate the effect of increasing the substrate temperature from 300 to 500°C at fixed pressure of 0.5 mbar and power of 150W. The increase in the growth rate can be explained by an enhanced dissociation of TMGa at the substrate level. When fixing the temperature at 500 °C, adding a SiN interface layer (S4) or even reducing the pressure to 0.3 mbar (S5) did not affect the growth rate, while a significant improvement was observed by increasing the RF power from 150 to 200 W (S6), nearly doubling the deposition rate. At 200 W, further increment in substrate temperature to 550°C (S7) and 600°C (S8) leads to the increase of the growth rate, likely due to improved thermally activated TMGa dissociation. In the same way, further increasing the RF power to 250 W (S9) and 300 W (S11) resulted in even higher deposition rate close to 0.7 µm/h. Finally, we choose the process conditions of S9, represented with a green circle in **Figure 2**. This particular set of conditions enabled us to achieve a reasonable growth rate of 0.55 µm/h while having a film that exhibits the best characteristics in terms of crystalline quality. The properties of the GaN film resulting from this process conditions are further discussed in the subsequent sections of this paper.

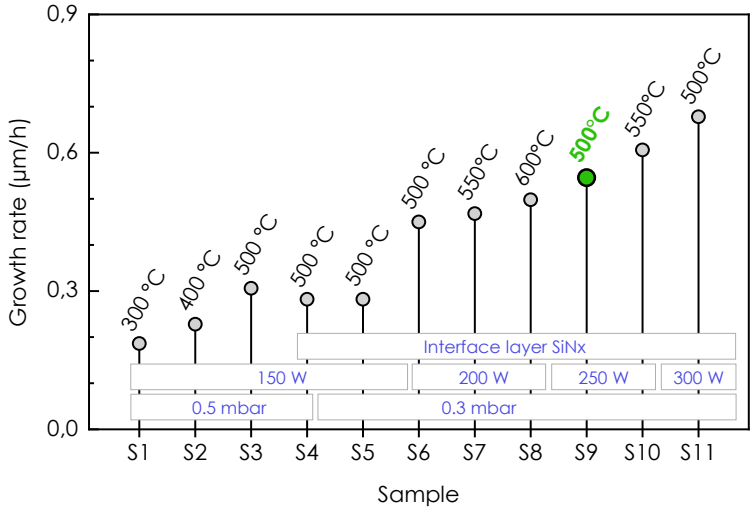

Figure 2. Optimization of growth conditions with parameter-by-parameter effect on growth rate.

C. Characterization techniques

To qualify the plasma source, Optical Emission Spectroscopy (OES) was performed using an AVANTES Avaspec-ULS4096 CL-EVO. This was mainly applied to identify the species in the plasma in a qualitative manner and to identify the conditions at which the E to H mode transition occurs[27]. To analyse the microstructure of the films, we used an X-ray diffractometer (XRD) Empyrean from Panalytical [CuK_α radiation λ = 1.5406 Å]. Spectroscopic ellipsometry (SE) was employed to determine the thickness and optical properties of the deposited layers. The measurements were performed using a Horiba Jobin Yvon UVISEL 2 and, subsequently, the data were processed using the DeltaPsi2© software. To gain information on the morphological and topographical features of the films, we used a Scanning Electron Microscope (SEM) – Merlin Compact from Zeiss and an Atomic Force Microscope (AFM) PicoScan 3000 (resolution XY: 1nm, Z < 1nm) from Agilent, respectively. As far as the chemical composition is concerned, ion beam analyses (IBA) using a 4MV Van De Graff accelerator (HVEE, KN4000) at ICube in Strasbourg were performed. Rutherford Backscattering Spectrometry (RBS) was used to determine the gallium content. RBS experiments were carried out with a 2 MeV alpha particle beam (He+) with a scattering angle of 160°. To determine the concentration of the low-Z elements (nitrogen,carbon and oxygen impurities), Nuclear Reaction Analysis (NRA) were performed using a 900 keV deuteron beam (H^{2+}) with a scattering angle of 150°. Under these conditions, light elements (C, N and O) were detected simultaneously in a single measurement.

III. RESULTS AND DISCUSSION

A. Plasma analysis

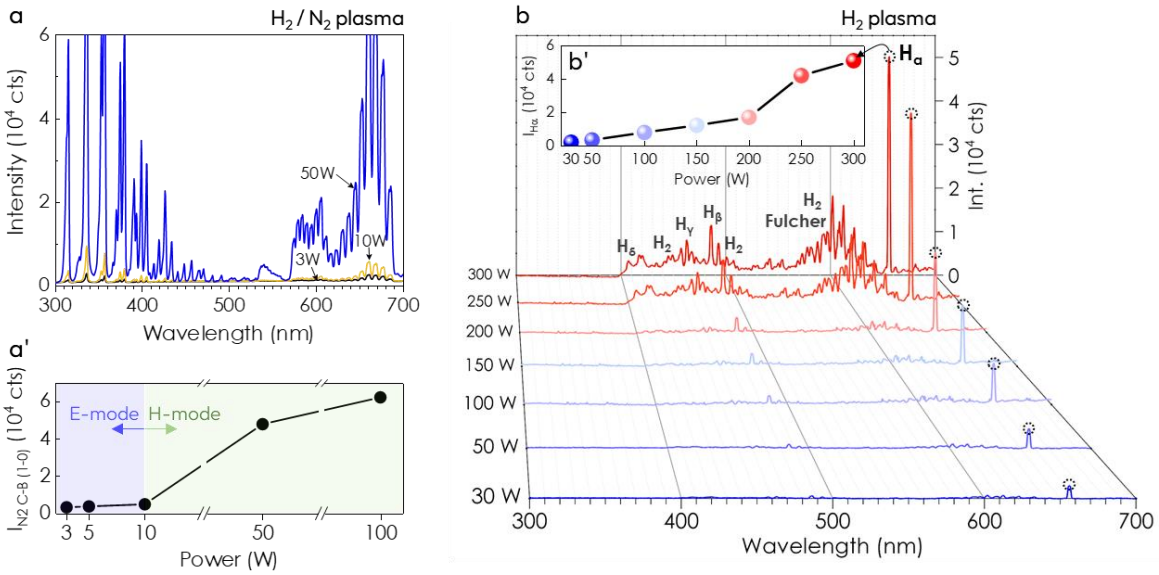

Figure 3. Optical emission spectra of (a) H_2/N_2 (1:40) plasma at 3 W, 10 W and 50 W under a total pressure of 0.3 mbar, (a') N_2 C-B (1-0) line tracking as a function of plasma power to identify the E-H transition, (b) a pure H_2 plasma at different plasma powers and (b') H_α line tracking as a function of plasma power.

The ICP plasma is generated in a mixture of nitrogen and hydrogen so that N-atoms and NH_x radicals can be produced[28]. In ICP-RF plasma sources, a transition between operational modes occurs, shifting from a low-power mode primarily characterized by capacitive coupling (E-mode) to a high-power mode where inductive coupling dominates (H-mode)[27]. The latter is characterized by a high plasma density, which is of particular interest for improving N_2 dissociation[24]. For this purpose, we searched for the condition required to reach this transition using OES by focusing on plasma power effect. **Figure 3 (a)** represents the optical emission spectrum of H_2/N_2 plasmas at 3 W, 10 W and 50 W. Above 10 W, we observe a jump in emission intensities as illustrated in **Figure 3 (a')**, such an increase of the light emission was even visible to the naked eye. Therefore, we set a

power value greater than 50 W to ensure an inductive mode that would promote higher N-atoms production.

The determination of the adequate plasma power value for the deposition process requires further analysis at extended power range especially if high growth rate is targeted. For this purpose, OES spectra were captured at RF power values spanning from 30 to 300 W (**Figure 3 (b))** with a focus on the H_α atomic hydrogen line intensity (**Figure 3 (b'))**. These results clearly show that H line monotonically increase from 30 to 200 W after which point a drastic increase is observed. It happens that this trend aligns with the enhanced growth rate for power greater than 200 W (see **Figure 2**) along with a reduction in carbon contamination, as it will be described later in the article. In addition, we found that such high-power values enable the growth of better quality GaN films in terms of crystallinity. Thus, RF power was identified as the main parameter that drives the growth process in two manners: (i) promoting atomic nitrogen generation that contributes to high growth rate of GaN films, while (ii) generating atomic hydrogen which helps in etching carbon contamination from the growth surface.

B. Thin film properties

1. Film crystallinity

Figure 4 shows the X-ray diffraction pattern in the Bragg-Brentano geometry of a GaN thin film grown under the working conditions of S9 given in **Table 1**. It presents a main peak at 34.2°, corresponding to the (0002) characteristic peak of GaN in the wurtzite structure. The additional peaks between 45° and 60° originate from forbidden reflections

of the silicon substrate[29] and/or source contamination. This shows that the films have a well-defined texture with all grains oriented in the c direction.

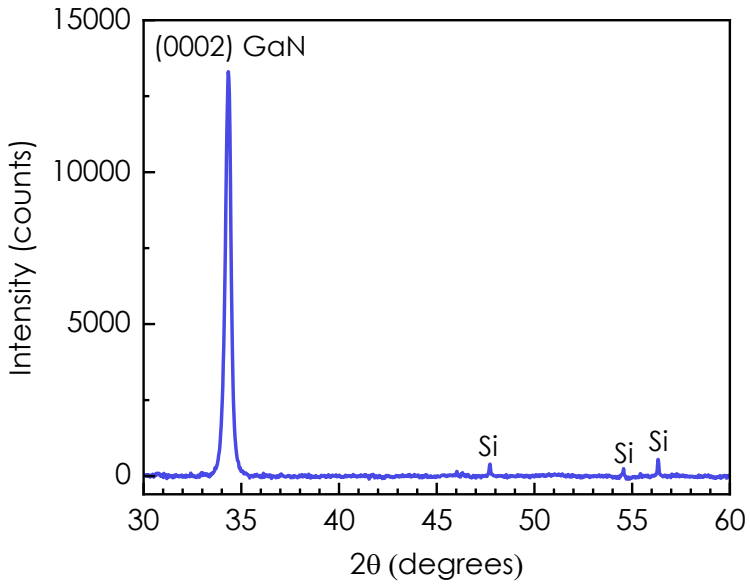

Figure 4. XRD spectrum of a GaN thin film grown by remote-plasma CVD. *Operating conditions of sample S9 (see Table 1).*

The average crystallite size has been calculated using the Scherrer formula given in **Equation (1)** where D is the average crystallite size in nm, *IB* the integral breadth, *K* is a numerical factor frequently described as the crystallite form factor or Scherrer constant (here K=1.07 corresponding to a spherical crystallite for a calculation with IB), λ is the incident wavelength ($\lambda = 1.54$ Å, Cu-K_α radiation), θ_{hkl} the Bragg diffraction angle of the corresponding (hkl) plane. The integral breadth (IB) is a measurement of the peak width. To calculate IB_{film} in **Table 2**, corresponding to the GaN (0002) peak, one has to consider the artefacts induced by the equipment (slit size, instrumental width...). For this purpose, another value, the instrumental integral breadth (IB_{instru}) is introduced and obtained by measuring a reference peak on the Si substrate. Fortunately, unlike the case of

diffraction from powder sample, IB_{instru} is independent of the angle. The instrumental width is subtracted from the total width and a corrected IB value of the GaN film is obtained (see **Table 2**). Finally, an average crystallite size of 97 nm has been calculated.

$$D = \frac{K\lambda}{IB\ cos\ \theta_{hkl}} \qquad (1)$$

Parameters						
K	λ (Å)	Peak position 2θ (°)	IB totale (°)	IB instru (°)	IB film (°)	D (nm)
1.07	1.54	34.24	0.20	0.10	0.10	97.95

Table 2 Crystallite size calculation from Scherrer formula. *Operating conditions of sample S9 (see Table 1).*

Figure 5 shows the real and imaginary parts of the pseudo-dielectric function of the sample S9 from ellipsometry measurement**.** The experimental data were fitted using a Tauc-Lorentz dispersion function (**Equation (2)**) and the layer stack presented in the inset, where a thin SiN interfacial layer of 17 Å was added between the c-Si substrate and the grown layer. This layer results from the nitridation treatment detailed earlier. Its thickness value was determined using elliposmetry performed on the c-Si wafer exposed to a H_2-N_2 plasma prior to GaN deposition. On top of the SiN layer, a layer of GaN corresponding to the bulk material and a second layer of GaN coupled with voids to simulate the roughness of the film via Effective Medium Approximation (EMA) were used. The experimental data could be reproduced by the optical model with the following fitting parameters: an optical bandgap E_g of 2.06 eV, an amplitude A of 54, a resonant energy E_0 of 5.13 and a disorder

parameter C of 3.29. From this simulation, a GaN thickness of 550 nm, having a surface roughness of 10 nm, was deduced.

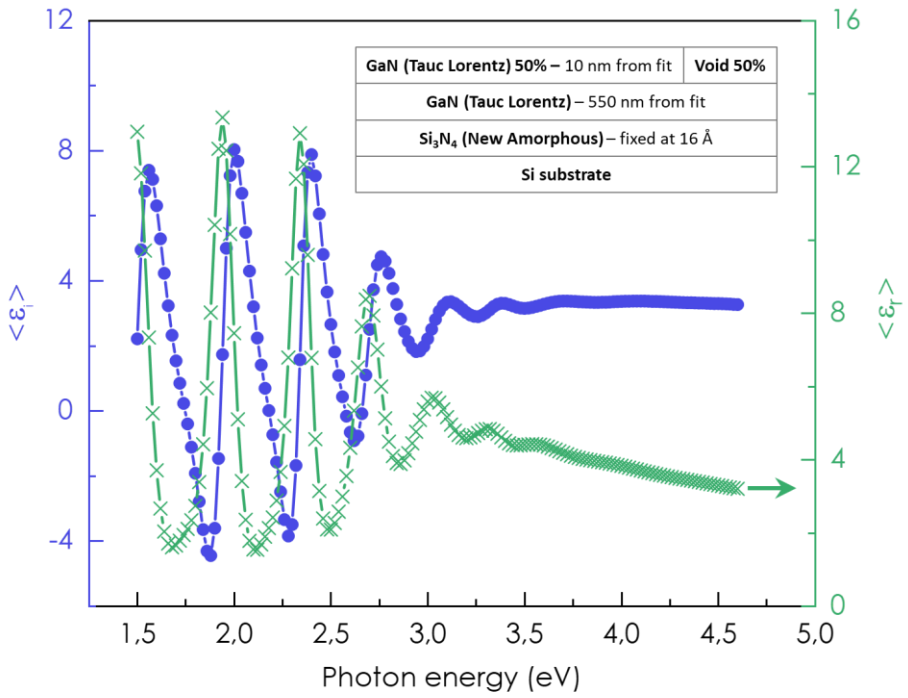

Figure 5. Ellipsometry measurement of GaN-on-Si by RP-CVD with the corresponding optical model (layer stack) used to fit the data. Operating conditions of sample S9 (see Table 1).

$$\varepsilon_2(E) = \frac{AE_0C(E-E_g)^2}{(E^2-E_0^2)^2+C^2E^2}\frac{1}{E} \quad (E > E_g) \qquad \varepsilon_2(E) = 0 \quad (E \leq E_g) \qquad (\mathbf{2})$$

2. *Morphological and topographical features*

Figure 6.a shows the cross-sectional SEM micrograph of a GaN film on Si. The GaN film exhibits a columnar structure with well-defined boundaries. As GaN has a large lattice mismatch with silicon (26%), it inevitably leads to the formation of a structure of

slightly misoriented sub-grains. We should mention that the thickness extracted from SEM, i.e. ~550 nm) is consistent with ellipsometry measurement (**Figure 5)**. The top-surface morphology is shown in **Figure 6 (b)** It reveals grains that are fairly uniform in size. For confirmation, a statistical analysis of the grain size was conducted using ImageJ software[30]. The corresponding Gaussian distribution is shown in **Figure 6 (b')** along with an insert showing the resulting parameters of the analysis. The average grain size is around 94 nm, which is in good agreement with the 97 nm crystallite size calculated from X-ray diffraction (**Table 2**). This means that overall, within each grain, a coherent crystalline orientation is achieved. As for topographical aspects, AFM measurements on the GaN film reveal a relatively smooth surface with a root mean square (RMS) roughness of 6.5 nm in the scanning area of 6.25μm^2 as shown in **Figure 6 (c)**, a value very close again to the one obtained with ellipsometry.

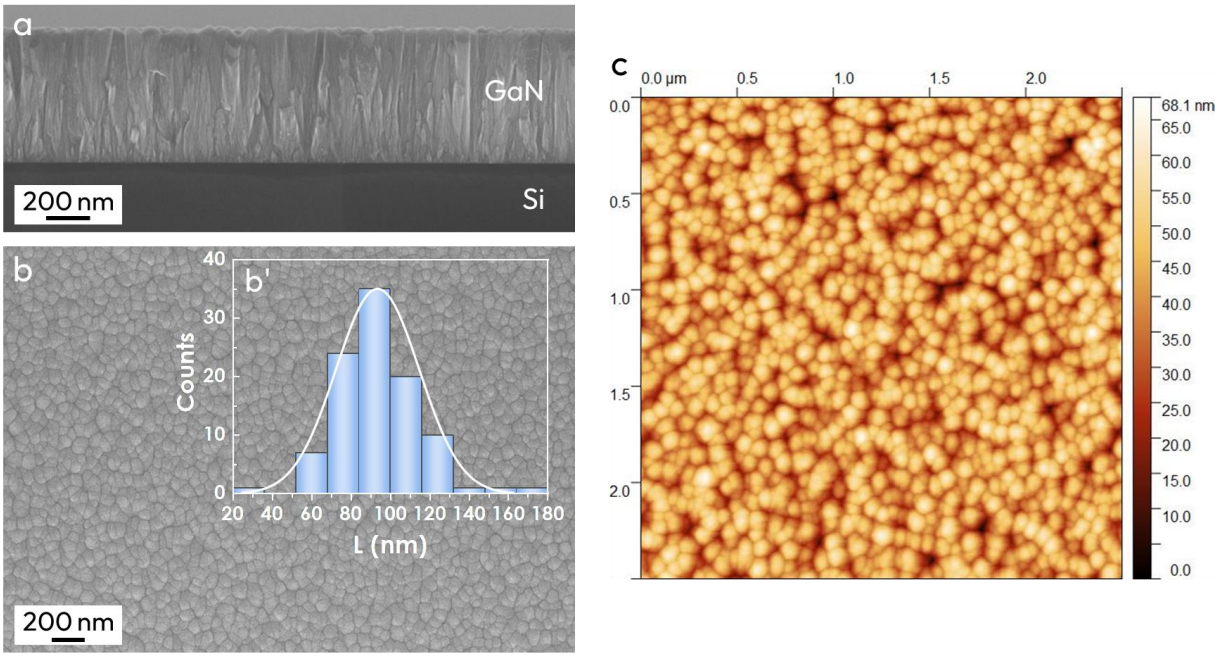

Figure 6. Cross-section (a) and top-view (b) SEM images of a 550 nm thick GaN film on c-Si, (b') statistical distribution of the grain size and (c) AFM image of the GaN thin film. *Operating conditions of sample S9 (see Table 1).*

3. GaN polarity

As our GaN films have a wurtzite structure and exhibit a growth strongly oriented along the polar axis c, we can determine the polarity (+c or -c) of the film by revealing it through chemical etching. The anisotropic KOH (potassium hydroxide) etchant is commonly used to reveal the polarity of GaN. For this purpose, we diluted KOH pellets in purified water as the high dielectric constant of water allows KOH to polarise into K^+ and $(OH)^-$ which oxidise the atoms in the GaN film[31]. A 1 M solution of KOH was heated to 70°C with a gentle magnetic stirring. Once the temperature of the solution was stabilized, the GaN sample was dipped into the solution for 5 minutes. It was then thoroughly rinsed in three baths of deionized water to ensure that all residual KOH was removed and dried in nitrogen atmosphere. The surface appearance before and after etching was investigated using SEM as shown in **Figure 7 (a)** and (**b)**, respectively. Overall, the KOH treatment did not induce major changes on the morphology when comparing **Figure 7 (a)** and (**b)**, except for minor modifications coming from classical etching, i.e. reduction of the grain size. Therofre, one may conclude that the film is Ga-polar (i.e., +c plane oriented or metal polar). Indeed, hydroxide ions etch the Ga atoms but are repelled by the electronegativity of the N dangling bond. In consequence, the morphology of Ga-polar surfaces is preserved while films with N-polar surfaces would have been modified with the appearance of pyramids over the entire surface corresponding to planes etched. This Ga-oriented polarity is the one usually obtained when producing smooth epitaxial thin films by conventional CVD. Moreover, it confers to the film some interesting properties for the bulk to be developed for various applications (e.g.: FETs, quantum wells) and especially a high chemical stability[32].

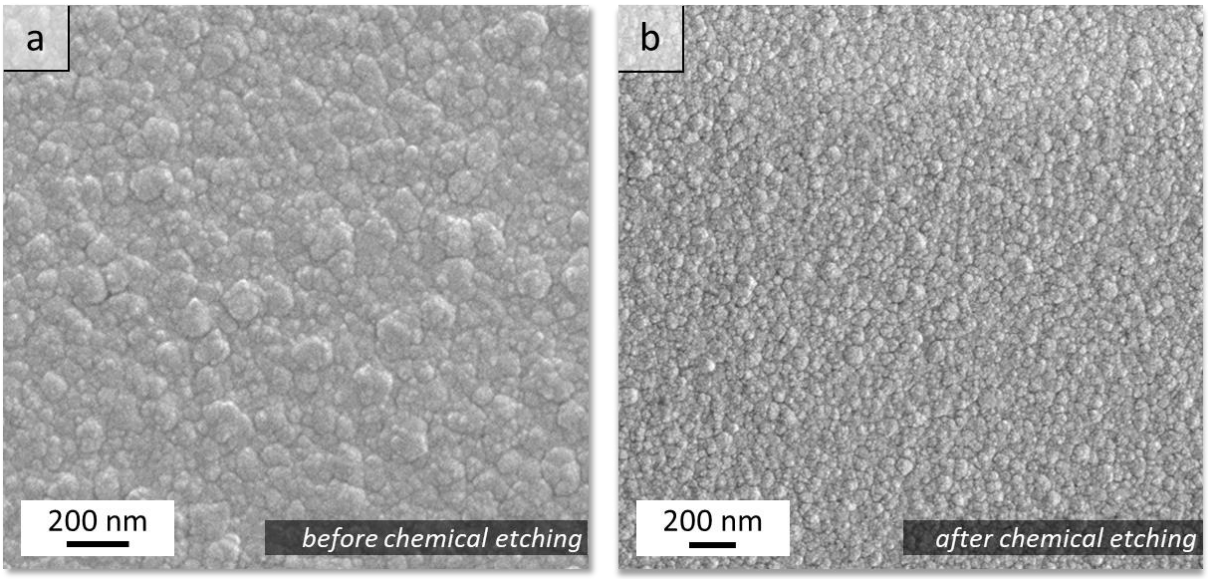

Figure 7. SEM surface image (a) before and (b) after KOH etching on GaN thin film by RP-CVD.

4. Chemical composition

Several methods exist in literature to analyze the chemical composition of materials, yet most are not well-suited for accurately quantifying GaN due to various limitations (such as the lack of calibration sample and nitrogen being a low-Z element). Consequently, we opted for IBA analyses, enabling direct quantification of the material without relying on fittings or calibration samples. To determine the in-depth composition of the GaN films, we employed a combination of two IBA techniques: RBS was used to examine gallium, a high-Z element, while NRA was employed to check the distribution of low-Z elements, specifically nitrogen, oxygen, and carbon impurities. The analyses first showed that oxygen content was extremely low, falling below the detection limit of NRA, which is typically on the order of 1%. This achievement can be attributed to the walls and substrate cleaning plasma treatment performed in the reactor before the growth process. We combined the results obtained from NRA and RBS to generate the depth profile of Ga,

N, and C within a GaN layer as shown in **Figure 8**. It reveals that the chemical composition of each element remains rather constant within the layer's depth, despite some minor variations observed in the nitrogen composition coming from the higher error associated with its measurement, i.e. ± 10%. Also, the spread of the N profile towards negative values is attributable to the depth resolution, which is closely linked to the energy resolution of the detector. A significant observation derived from this graph is the stoichiometric nature of the GaN film, presenting a Ga/N ratio close to 1 consistently across the entire depth of the film.

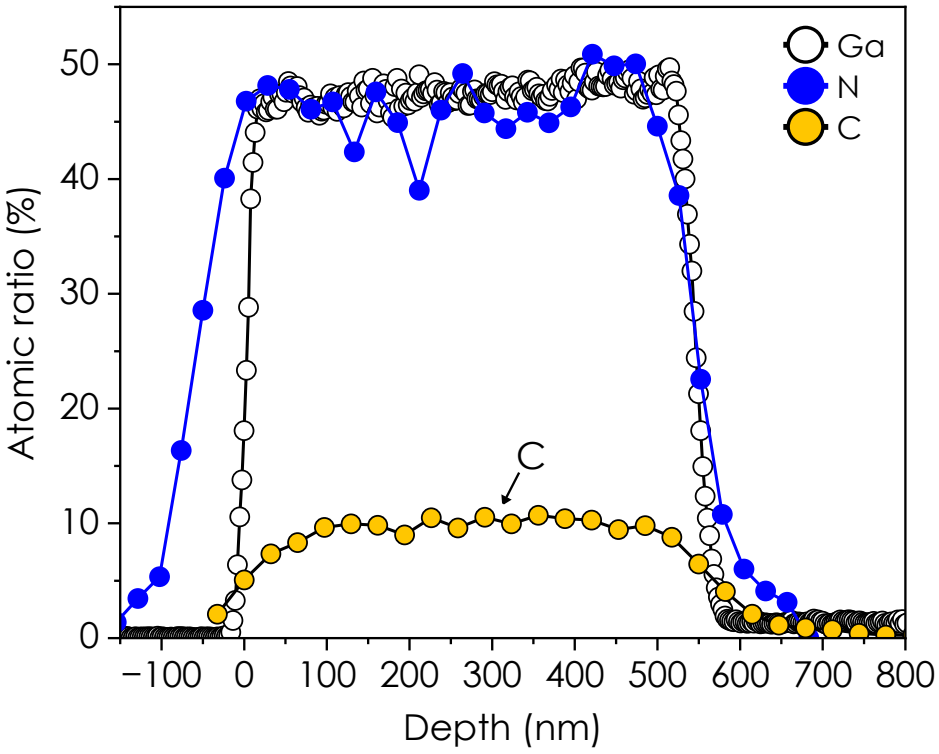

Figure 8. Plot of combined RBS-NRA in-depth profile of GaN on Si by RP-CVD. *Operating conditions of sample S9 (see Table 1).*

However, the film presents a carbon content as high as 10% (originated from TMGa decomposition). To reduce the carbon impurities, a possible route investigated here, was to increase the H_2 dissociation in the ICP source by increasing the RF power so that a higher density flux of H-atoms would promote the etching of C from the growing surface. Indeed, as previously shown in **Figure 3**, the increase of the RF power induces a large increase in the intensity of atomic emission lines of H, especially above 150 W. **Figure 9** illustrates the influence of the RF plasma power on the film composition where Ga/N ratio as well as C atomic percentage are shown. It should be noted that concentrations depicted here reflect the average concentration across the layer, encompassing both surface and interface influences. This figure highlights that higher plasma power leads to reduced carbon contamination, with C content dropping from 11.5% to ~7.5%, by varying the power from 150 to 300 W. As mentioned before, this would likely result from the higher density of reactive atomic hydrogen that undergoes gas-phase and, most importantly, surface reactions leading to removal of carbon atoms and binding them into stable carbon-containing species, thus leading to a decrease in carbon incorporation during the growth[33,34]. Interestingly, the increase in H-atoms density does not influence the Ga and N concentration in the films, which is a valuable aspect of this process as one may tune the density of C in the layer without affecting the Ga/N ratio.

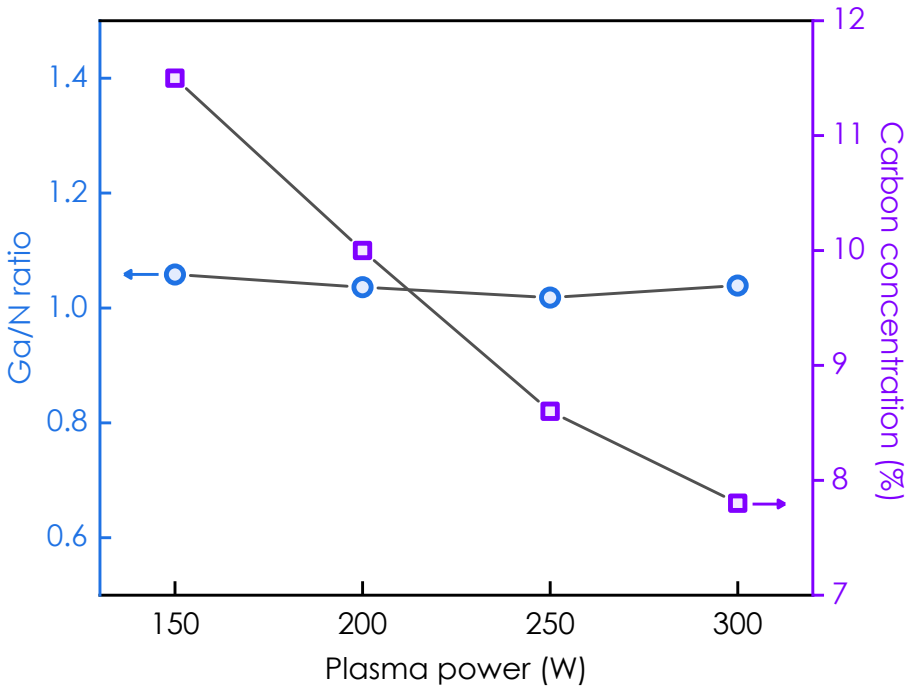

Figure 9. Carbon concentration and III/V ratio over the thickness of the GaN layer as a function of RF plasma power from combined NRA and RBS analyses. *Operating conditions of sample 9 except for the RF power (see Table 1).*

IV. SUMMARY AND CONCLUSIONS

In conclusion, our study successfully demonstrated the low-temperature and low-pressure growth of highly textured GaN thin films on crystalline silicon substrates using RP-CVD. Using the custom-designed reactor, the generation of a remote plasma operating in the inductive mode effectively facilitated the decomposition of the group-V precursor N_2, supplemented by H_2 whose efficient dissociation allows to reduce the carbon contamination in the layer from 11.5% down to 8% when RF power was increased from 150 to 300 W without affecting the Ga/N ratio. Notably, the layers are quasi-stoichiometric across the film's depth, emphasizing their uniformity while being almost free of O (less

than 1% at., i.e. the detection limit of NRA). The investigations have established that GaN layers have a well-defined texture with most of the grains oriented in the +c direction, with a highly dense columnar structure. These films displayed nanometer-scale roughness, with uniform grain sizes in the hundred-nanometer range, consistent with the crystallite size of 98 nm determined from XRD analysis. These results pave the way for a growth technique that aligns with the cost-effective production of III-V thin films, through minimized gas consumption which is facilitated by the low-pressure operation of RP-CVD.

ACKNOWLEDGMENTS

This project has been supported by the French Government in the frame of the program of investment for the future (Programme d'Investissement d'Avenir - ANR-IEED-002-01).

REFERENCES

[1] S. Nakamura, T.M.T. Mukai, and M.S.M. Senoh, "High-Power GaN P-N Junction Blue-Light-Emitting Diodes," Jpn. J. Appl. Phys. **30**(12A), L1998 (1991).
[2] S. Strite, and H. Morkoç, "GaN, AlN, and InN: A review," Journal of Vacuum Science & Technology B: Microelectronics and Nanometer Structures Processing, Measurement, and Phenomena **10**(4), 1237–1266 (1992).
[3] E. Monroy, E. Muñoz, F.J. Sánchez, F. Calle, E. Calleja, B. Beaumont, P. Gibart, J.A. Muñoz, and F. Cussó, "High-performance GaN p-n junction photodetectors for solar ultraviolet applications," Semicond. Sci. Technol. **13**(9), 1042 (1998).
[4] M.A. Würtele, T. Kolbe, M. Lipsz, A. Külberg, M. Weyers, M. Kneissl, and M. Jekel, "Application of GaN-based ultraviolet-C light emitting diodes – UV LEDs – for water disinfection," Water Research **45**(3), 1481–1489 (2011).
[5] A.Y. Polyakov, S.J. Pearton, P. Frenzer, F. Ren, L. Liu, and J. Kim, "Radiation effects in GaN materials and devices," J. Mater. Chem. C **1**(5), 877–887 (2013).
[6] N. m Nasser, Z. Ye Zhi, J. Li, and B. Xu Ya, "GAN HETEROEPTAXIAL GROWTH TECHNIQUES," Journal of Microwaves, Optoelectronics and Electromagnetic Applications (JMOe) **2**(3), 22–31 (2001).
[7] H. Randhawa, "Review of plasma-assisted deposition processes," Thin Solid Films **196**(2), 329–349 (1991).

[8] K.A. Horowitz, T.W. Remo, B. Smith, and A.J. Ptak, *A Techno-Economic Analysis and Cost Reduction Roadmap for III-V Solar Cells* (2018), p. NREL/TP--6A20-72103, 1484349.
[9] P. Roca i Cabarrocas, "Plasma enhanced chemical vapor deposition of amorphous, polymorphous and microcrystalline silicon films," Journal of Non-Crystalline Solids **266–269**, 31–37 (2000).
[10] K. Ouaras, S. Filonovich, B. Bruneau, J. Wang, M. Ghosh, and E. Johnson, "Maskless interdigitated a-Si:H PECVD process on full M0 c-Si wafer: Homogeneity and passivation assessment," Solar Energy Materials and Solar Cells **246**, 111927 (2022).
[11] G.L. Kabongo, B.M. Mothudi, and M.S. Dhlamini, "Advanced Development of Sustainable PECVD Semitransparent Photovoltaics: A Review," Front. Mater. **8**, 762030 (2021).
[12] K.P. Pande, and A.C. Seabaugh, "Low Temperature Plasma-Enhanced Epitaxy of GaAs," J. Electrochem. Soc. **131**(6), 1357 (1984).
[13] Q. Liang, R.-Z. Wang, M.-Q. Yang, Y. Ding, and C.-H. Wang, "A green, low-cost method to prepare GaN films by plasma enhanced chemical vapor deposition," Thin Solid Films **710**, (2020).
[14] A.S. Gudovskikh, I.A. Morozov, A.V. Uvarov, D.A. Kudryashov, E.V. Nikitina, A.S. Bukatin, V.N. Nevedomskiy, and J.-P. Kleider, "Low temperature plasma enhanced deposition of GaP films on Si substrate," Journal of Vacuum Science & Technology A: Vacuum, Surfaces, and Films **36**(2), 021302 (2018).
[15] J. Emanuel Thomet, A. Kamlesh Singh, M. Nelly Rouèche, N. Toggwyler, F.-J. Haug, G. Christmann, S. Nicolay, C. Ballif, N. Wyrsch, A. Hessler-Wyser, and M. Boccard, "Bandgap engineering of indium gallium nitride layers grown by plasma-enhanced chemical vapor deposition," Journal of Vacuum Science & Technology A **40**(6), 063102 (2022).
[16] M. Khoury, O. Tottereau, G. Feuillet, P. Vennéguès, and J. Zúñiga-Pérez, "Evolution and prevention of meltback etching: Case study of semipolar GaN growth on patterned silicon substrates," Journal of Applied Physics **122**(10), 105108 (2017).
[17] M. Losurdo, P. Capezzuto, and G. Bruno, "Remote plasma metalorganic chemical vapor deposition of GaN epilayers," J. Phys. IV France **09**(PR8), Pr8-799-Pr8-804 (1999).
[18] C. Martin, K.S.A. Butcher, M. Wintrebert-Fouquet, A. Fernandes, T. Dabbs, P.P.-T. Chen, and R. Carmen, in edited by H. Morkoç, C.W. Litton, J.-I. Chyi, Y. Nanishi, and E. Yoon (San Jose, CA, 2008), p. 689407.
[19] G. Bruno, P. Capezzuto, and M. Losurdo, "Growth of InP in a Novel Remote-Plasma MOCVD Apparatus : an Approach to Improve Process and Material Properties," J. Phys. IV France **05**(C5), C5-481-C5-488 (1995).
[20] W.-C. Lai, C.-Y. Chang, M. Yokoyama, J.-D. Guo, J.-S. Tsang, S.-H. Chan, J.-S. Bow, S.-C. Wei, R.-H. Hong, and S.M. Sze, "Epitaxial Growth of the GaN Film by Remote-Plasma Metalorganic Chemical Vapor Deposition," Jpn. J. Appl. Phys. **37**(10R), 5465 (1998).
[21] A. Dadgar, "Sixteen years GaN on Si: Sixteen years GaN on Si," Phys. Status Solidi B **252**(5), 1063–1068 (2015).
[22] S. Guha, and N.A. Bojarczuk, "Ultraviolet and violet GaN light emitting diodes on silicon," Applied Physics Letters **72**(4), 415–417 (1998).

[23] S. Guha, and N.A. Bojarczuk, “Multicolored light emitters on silicon substrates,” Applied Physics Letters **73**(11), 1487–1489 (1998).
[24] T.L. (Tom L. Cottrell, “The strengths of chemical bonds,” (No Title), (n.d.).
[25] T. Czerwiec, F. Greer, and D.B. Graves, “Nitrogen dissociation in a low pressure cylindrical ICP discharge studied by actinometry and mass spectrometry,” J. Phys. D: Appl. Phys. **38**(24), 4278–4289 (2005).
[26] K. Nakashima, M. Ishii, I. Tajima, and M. Yamamoto, “Existence of threshold density in silicon surface cleaning using hydrogen electron cyclotron resonance plasma,” Applied Physics Letters **58**(23), 2663–2665 (1991).
[27] U. Kortshagen, N.D. Gibson, and J.E. Lawler, “On the E - H mode transition in RF inductive discharges,” J. Phys. D: Appl. Phys. **29**(5), 1224 (1996).
[28] Y. Lu, H. Kondo, K. Ishikawa, O. Oda, K. Takeda, M. Sekine, H. Amano, and M. Hori, “Epitaxial growth of GaN by radical-enhanced metalorganic chemical vapor deposition (REMOCVD) in the downflow of a very high frequency (VHF) N2/H2 excited plasma – effect of TMG flow rate and VHF power,” Journal of Crystal Growth **391**, 97–103 (2014).
[29] P. Zaumseil, “High-resolution characterization of the forbidden Si 200 and Si 222 reflections,” J Appl Crystallogr **48**(2), 528–532 (2015).
[30] C.A. Schneider, W.S. Rasband, and K.W. Eliceiri, “NIH Image to ImageJ: 25 years of image analysis,” Nat Methods **9**(7), 671–675 (2012).
[31] M. Tautz, and D. Díaz Díaz, “Wet-Chemical Etching of GaN: Underlying Mechanism of a Key Step in Blue and White LED Production,” ChemistrySelect **3**(5), 1480–1494 (2018).
[32] E.S. Hellman, “The Polarity of GaN: a Critical Review,” MRS Internet j. Nitride Semicond. Res. **3**, e11 (1998).
[33] C. Sone, M. Hong Kim, H. Jin Kim, and E. Yoon, “Effects of hydrogen on carbon incorporation in GaN grown by remote plasma-enhanced metal-organic chemical vapor deposition,” Journal of Crystal Growth **189–190**, 321–324 (1998).
[34] M. Masi, H. Sirnka, K.F. Jensen, and T.F. Kuech, “Simulation of carbon doping of GaAs during MOVPE,” (n.d.).